JOURNAL OF OPTOELECTRONICS AND ADVANCED MATERIALS, Vol. 12, No. 5, May 2010, p. 1206 - 1212

Protein attachment on aluminosilicates surface studied by XPS and FTIR spectroscopy

E. VANEA, K. MAGYARI, V. SIMON*
Babes-Bolyai University, Faculty of Physics & Institute of Interdisciplinary Research in Bio-Nano-Sciences, Cluj-Napoca, Romania

Bovine serum albumin and fibrinogen attachment on aluminosilicate samples with biomedical potential was tested as major plasma proteins which are adsorbed on the surface of blood contact biomaterials. The samples were incubated for 2 hours in simulated body fluid with bovine serum albumin and buffered fibrinogen solution. Proteins attachment on the surface of the investigated samples is reflected by the presence of the N 1s photoelectron peak and by the modification in the C 1s core-level signal in the XPS spectra of the samples treated with protein solution. The results obtained from FTIR analysis of amide I vibrations were correlated with the secondary structure of the proteins attached on investigated sample surface.

(Received April 1, 2010; accepted May 26, 2010)

*Keywords:*Protein, Aluminosilicate, XPS, FTIR

1. Introduction

The study of protein-material surface interactions represents one of the most important topics in the field of biomaterials for several decades [1]. The reason for the great interest in this topic is due to the fact that protein-surface interactions are fundamentally responsible for the biocompatibility of medical devices, because when a solid material comes in contact with a fluid that contains soluble proteins, e.g., blood, interstitial fluid, cell culture media, proteins rapidly adsorb onto the surface of the material, saturating the surface within a time frame of seconds to minutes [2]. Protein adsorption and subsequent changes in their conformation are primary interactions of a biological environment with foreign surfaces [3]. When living cells, which are much larger than proteins and thus much more slowly moving, approach the biomaterial surface, they do not actually contact the molecular structure of the material surface itself, but rather they contact and interact with the molecular structure of the adsorbed protein layer. The cells perceive their surrounding by means of membrane receptors that can bind to specific bioactive features presented by the adsorbed proteins, and these receptor-protein binding events determine the cells response. The cellular response can be controlled by the adsorbed layer of proteins [4, 5**].**

Albumin and fibrinogen are two main components of blood plasma. The ratio between human serum albumin and fibrinogen is normally 10:1 [6]. The attachment of these proteins on the surface of blood contact biomaterials strongly affect their biocompatibility [7, 8]. Albumin is a globular protein, has the molecular mass of 67 kDa, and is the predominant plasma protein, making up 60-70% of plasma [9]. In human serum the albumin is present at concentrations in the range of 35 to 45 mg/ml [10] and it has been found that its adsorption on surfaces inhibits thrombus formation [11, 12]. Albumin is generally considered to passivate the surface and greatly reduce the acute inflammatory response of the biomaterial [13]. Fibrinogen is a 340 kDa dimeric fibrous protein and its normal concentration in human blood is in the range of 2 to 4 mg/ml [14]. Fibrinogen adsorption is one of the initial events that occur when biomaterials come into intimate contact with blood [15]. Therefore, the tendency to adsorb fibrinogen appears to be an indicator of biocompatibility.

The aluminosilicate glass ceramics are highly stable in the body and by addition of iron and yttrium oxides they could be optimised for hyperthermia and radiotherapy applications [16-21]. The modifications on the surface of biomaterials are expected to ensure the biocompatiblity and stability against defence system of the body, permitting their long term maintenance in organism.

X-ray Photoelectron Spectroscopy (XPS) yields information concerning the atomic composition and chemical environment of the first 2-10 nm layer of a material surface and can accurately determine the surface coverage. Fourier Transform Infrared Spectroscopy (FTIR) is one of the most used techniques for studying protein secondary structures.

The present study aims to investigate the interaction of bovine serum albumin and fibrinogen with an aluminosilicate system containing iron and yttrium, for further biomedical applications. XPS and FTIR spectroscopy were used to investigate the proteins adsorption after 2 hours of sample immersion *in vitro* in protein solutions.

2. Materials and methods

Bovine serum albumin (BSA, fraction V) and fibrinogen (type I-S, from bovine plasma) were purchased from Fluka and respectively from Sigma-Aldrich, as lyophilised samples.

The 60SiO2·20Al2O3·10Fe2O3·10Y2O3 (mol %) system used in this study was obtained by sol-gel process.

The dried sample was calcinated at 1200 °C in air for 24 hours, milled and sieved to obtain particle size less than 60 μm.

Protein adsorption experiments were carried out by incubating the aluminosilicates sample in simulated body fluid (SBF) [22] with bovine serum albumin (BSA, 1mg/ml), and in fibrinogen solution prepared in phosphate–buffered saline solution (PBS, pH 7.2, 2 mg/ml). The samples immersed in these protein solutions were kept at 37°C in Incutherm RAYPA type incubator for 2 hours under static conditions. After 2 hours they were plenty rinsed with ultra pure water and filtered to ensure that any non-adsorbed protein molecules were removed. Then the samples were air-dried at 37°C for 24 hours.

XPS measurements were performed using a SPECS PHOIBOS 150 MCD system equipped with monochromatic Al-K_α source (250 W, hv=1486.6 eV), hemispherical analyser and multichannel detector. The typical vacuum in the analysis chamber during the measurements was in the range of 10^{-9}- 10^{-10} mBar. The binding energy scale was charge referenced to the C 1s at 284.6 eV. Elemental compositions were gdetermined from spectra acquired at pass energy of 100 eV. High-resolution spectra were obtained using analyser pass energy of 30 eV.

FTIR spectra of the samples were recorded in reflection configuration by a Jasco IRT-5000 FT-IR spectrometer in the range 4000-650 cm^{-1} with a resolution of 4 cm^{-1}.

3. Results and discussion

The XPS survey spectrum recorded before immersion (Fig. 1a) reveals only photoelectron peaks corresponding to the elements entering in the sample composition, and the C 1s photoelectron peak which usually is evidenced on all surfaces exposed to the atmosphere. The intensity decrease observed for the photoelectron peaks corresponding to Si, Al, Fe and Y substrate elements after sample immersion in protein solutions (Fig. 1b and 1c) is explained by surface coverage with proteins.

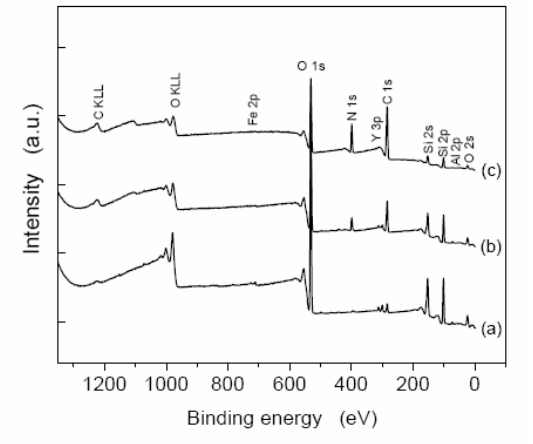

Fig. 1. XPS survey spectra before immersion (a), and after 2 hours immersion in BSA (b) and in fibrinogen (c) solutions.

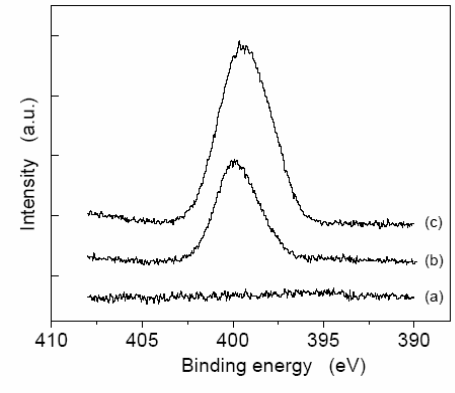

Fig. 2. N 1s high-resolution XPS spectra before immersion (a), and after 2 hours immersion in BSA (b) and fibrinogen (c) solutions.

At the same time, the presence of the intense XPS nitrogen peak for every functionalised sample means the nitrogen content can be used as a reliable marker for protein adsorption (Fig. 2). In addition, the deconvolution of N 1s core level spectra (Fig. 3) reveals two components at 398.2 and 400 eV, that are characteristic of C-NH_2 groups [23].

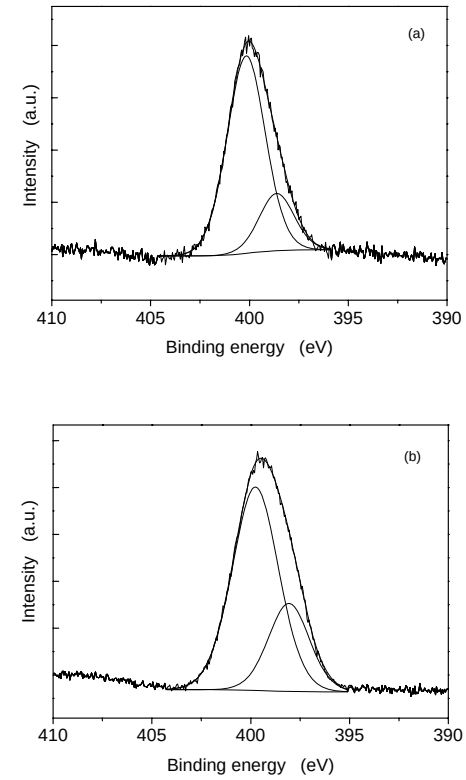

Fig. 3. Deconvoluted N 1s high resolution XPS spectra after 2 hours immersion in BSA (a) and fibrinogen (b) solutions.

Table 1. Elemental surface composition determined from XPS survey spectra before and after immersion of samples in BSA and fibrinogen solutions.

Sample	at %						
	C	N	O	Al	Si	Fe	Y
before immersion	6.92	-	53.08	2.3	36.77	0.18	0.75
immersed in BSA	28.93	6.46	37.21	1.71	25.2	0.03	0.46
immersed in fibrinogen	51.81	11.5	23.25	0.41	13.02	0.01	-

The elemental analysis also indicates a remarkable increase of carbon content after incubation, but both the carbon and nitrogen levels are higher on the surface of the sample immersed in fibrinogen solution than on the surface of the sample immersed in BSA solution (Table 1).

On the surface of the sample immersed in fibrinogen solution a content of 11.5 at % nitrogen occurs, while after immersion in albumin solution the nitrogen content is 6.46 %, due to the smaller size of the albumin protein, which would yield a protein layer of smaller thickness than the XPS sampling depth.

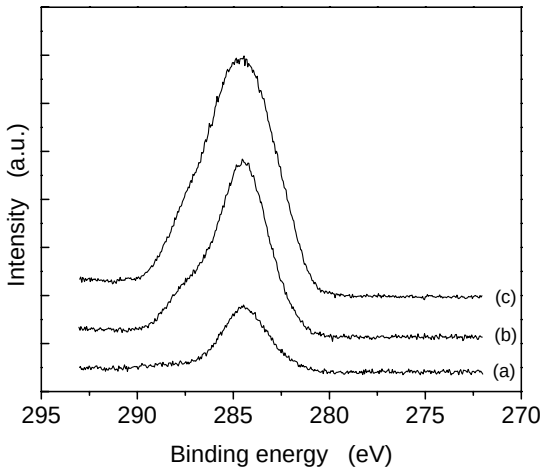

Fig. 4. C 1s high-resolution XPS spectra before immersion (a), after 2 hours immersion in BSA (b) and fibrinogen (c) solutions.

The high-resolution C 1s spectra (Fig. 4) show that C 1s photoelectron peaks are much broader after sample immersion in protein solutions. The analysis of the deconvoluted C 1s spectra (Fig. 5) shows that before immersion on the sample surface occur only contamination C-C and C-H species, giving rise to the sole component with binding energy 284.6 eV, representing the hydrocarbon (C-H), while after 2 hours immersion in protein solution beside the component of aliphatic carbon is well evidenced the component at about 288 eV corresponding to the C=O and –CONH- bonds of proteins [24, 25].

The O 1s high resolution spectra (Fig. 6) show that before immersion in protein solutions the O 1s photoelectron peak consists only of one component, at 532.2 eV, which is related to the oxygen occurring in sample structural units [26], and to a limited extend it could be assigned to hydroxyl groups incidentally present on the surface due to the chemisorbed water molecules from environmental moisture [27]. After immersion in BSA and fibrinogen solutions, the O 1s photoelectron peaks are broader, especially after immersion in fibrinogen solution. The full with at half maximum is 2.87 eV before immersion and becomes 2.95 eV after immersion in BSA solution and 3.79 eV after immersion in fibrinogen solution. Oxygen concentration also decreases on the surface of the samples immersed for 2 hours in protein solutions (Table 1), because large part of the oxide aluminosilicate sample is covered by protein molecules, which are less rich in oxygen atoms.

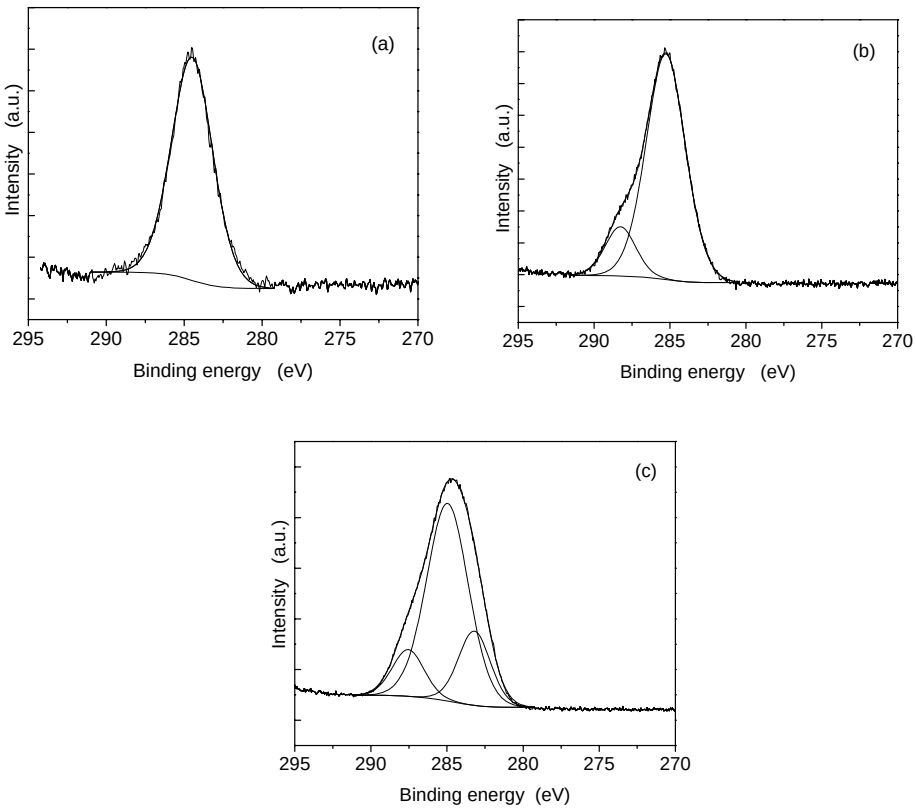

Fig. 5. Deconvoluted C 1s high resolution XPS spectra recorded before immersion (a), and after 2 hours immersion in BSA (b) and fibrinogen (c) solutions.

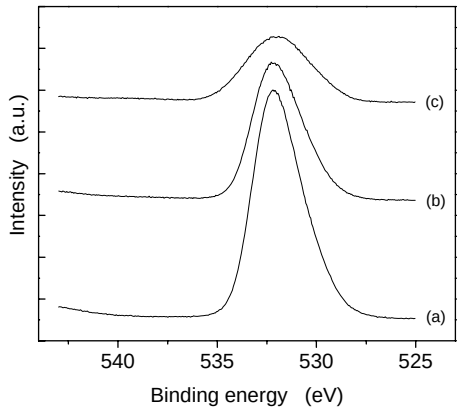

Fig. 6. O1s high resolution XPS spectra before immersion (a), after 2 hours immersion in BSA (b) and fibrinogen (c) solutions.

The infrared spectroscopy results were analysed with respect to protein secondary structure. The proteins exhibit characteristic bands, emerging from vibration in the peptide linkages, in 4000-1200 cm^{-1} spectral range of FTIR spectra. There are two dominant bands, namely amide I band (1600-1700 cm^{-1}) and amide II band around 1540 cm^{-1}. The amide I band is mostly used to extract information about the secondary structure. Because each of the different secondary structural elements contributes to the FTIR spectrum, the observed amide bands are composed of several overlapping components representing helices, β-structures, turns and random structures. Amide I (1600–1700 cm^{-1}) comprises contribution from 80% C=O stretching mode), Amide II (1500–1600 cm^{-1}: 60% N–H bending and 40% C–N stretching modes), Amide III (1200–1330 cm^{-1}: 40% C–N stretching and 30% N–H bending modes) [28, 29]. The exact frequency of the amide I vibration depends on the nature of the hydrogen bonding involving C=O and N-H groups, this in turn is determined by the particular secondary structure adopted by the protein [30, 31]. This band mainly involves the carbonyl stretching vibrations of the peptide backbone and it is a sensitive marker of peptide secondary structure, as the vibrational frequency of each C=O bond depends on hydrogen bonding and the interactions between the amide units [32]. The interpretation of the absorption bands recorded in this region requires that bands for α-helical structure overlap with those from random structure. Band deconvolution using the second derivative can be used to identify the number and the position of the bands underlying the amides envelops [3, 18, 33-35]. The amide I band was deconvoluted with a Gaussian line function after the position of the components was determined from

second derivative of FTIR spectra recorded from the lyophilized proteins and from the samples immersed in protein solutions. The assignements of the component bands were 1610-1640 cm^{-1} to β-sheet, 1640-1650 cm^{-1} to random coil, 1650-1658 cm^{-1} to α-helix and 1660-1700 cm^{-1} to β-turn structure [36]. The percentage of each component was calculated according to the coresponding integrated area.

The results obtained for liophylised BSA and BSA adsorbed on the material surface show that the conformation of BSA protein changes when it is adsorbed on material surface (Fig. 7). Compared to the lyophilised BSA, there are several conformation changes for the protein adsorbed on surface (Fig. 8) toward a higher β--sheet/β-turn ratio, which indicates protein-surface interaction and enhanced blood compatibility.

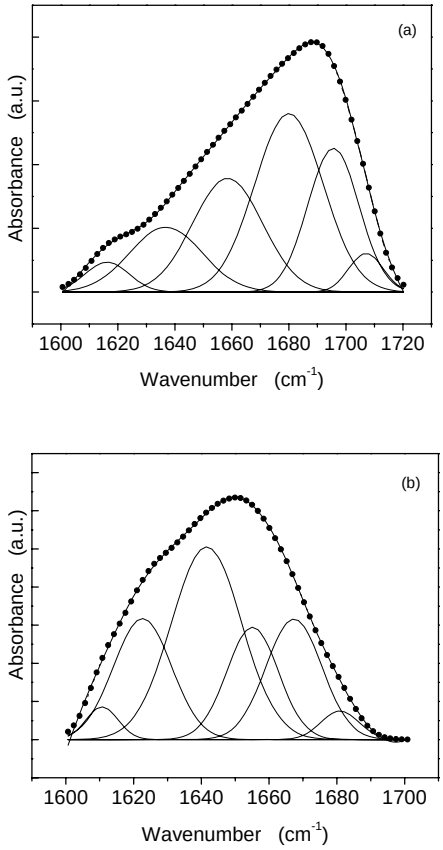

Fig. 7. Deconvolution of amide I absorption band of BSA - lyophilized powder (a); attached on aluminosilicate sample (b).

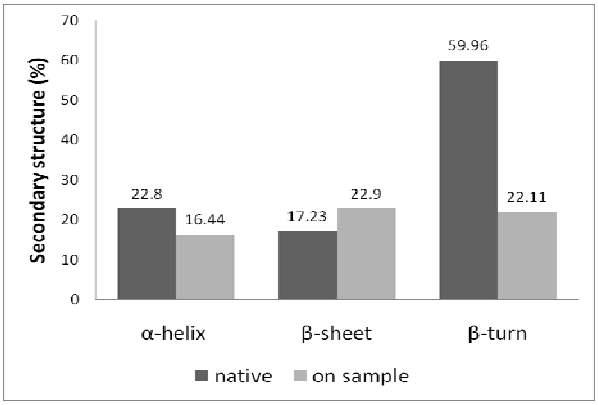

Fig. 8. Distribution of α-helix, β-sheet and β-turn secondary structures in lyophilised, and attached BSA.

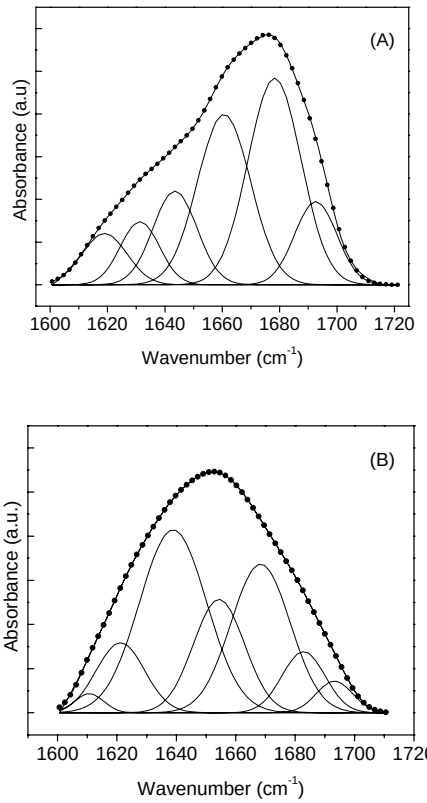

Fig. 9. Deconvolution of amide I absorption band of fibrinogen - lyophilized powder (a); attached on aluminosilicate sample (b).

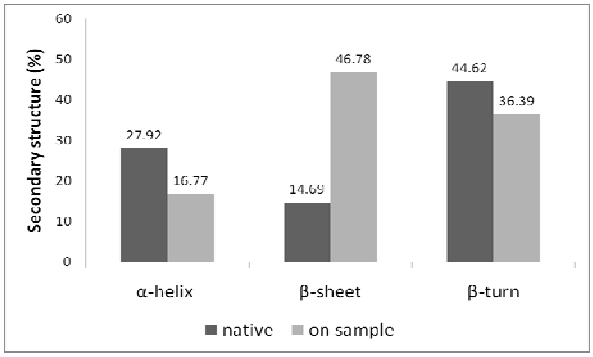

Fig. 10. Distribution of α-helix, β-sheet and β-turn secondary structures in lyophilised, and attached fibrinogen.

Fibrinogen adsorbed on material surface also changes its native structure. Deconvolution of the native fibrinogen (Fig. 9) amide I band was made assuming six components, and for the adsorbed fibrinogen the deconvolution was made assuming seven components.The α-helix content of adsorbed fibrinogen obviously decreases and is mainly transformed to β-sheet which meaningfully increases, while the β-turn is less changed.

One can observe from the data represented in Fig. 10 that β-sheet content increases from 14.69 % in lyophilized state to 46.78 % after adsorption on the investigated aluminosilicate sample. At the same time, after adsorption α-helix conformation decreases from 27.92 % to 16.77 % and the turns decrease from 44.62% to 36.39 %. However, it is not excluded that the 1640 cm^{-1} H-O-H bending vibration of water molecules adsorbed at the surface of the samples may also contribute to the intensity of the peak located around 1650 cm^{-1} [37].

The β-sheet/β-turns ratio used to indicate the biocompatibility of the biomaterial shows that this ratio exhibits a higher value for the adsorbed protein compared to the native one (Fig. 10), indicating a good biocompatibility of the material, as supported by other data in literature [3]. The changes in secondary structure of the proteins molecules could be determined by electrostatic interactions between positive charges of the protein and negative charges on biomaterial surface, and hydrogen bonding interaction [38].

4. Conclusions

XPS and FTIR results prove the attachment of BSA and fibrinogen on iron and yttrium containing aluminosilicate samples. Due to the proteins coating, the elemental analysis of XPS survey spectra evidences the occurrence of nitrogen present in the amino acids of the proteins.

On the surface of the sample immersed in fibrinogen solution a content of 11.5 at % nitrogen occurs, while after immersion in albumin solution the nitrogen content is 6.46 %, due to the smaller size of the albumin protein, which would yield a protein layer of smaller thickness than the XPS sampling depth. After immersion in protein solutions, the O1s photoelectron peaks are broadened, denoting the contribution of the peptidic oxygen.

FTIR absorption bands characteristic for proteins bring additional emphasis to the attachment of BSA and fibrinogen on sample surface. The secondary structure of amide I was analysed based on band deconvolution using the second derivative. The β-sheet/β-turns ratio exhibits a higher value for the adsorbed proteins compared to the native ones indicating a good biocompatibility of the material.

References

[1] T. S. Tsapikouni, Y.F. Missirlis, Mat. Sci. Eng. B-Solid **152**, 2 (2008).

[2] C. C. Berry, S. Adams, G. Curtis, J. Phys. D: Appl. Phys. **36**, R198 (2003).

[3] S. Tunc, M. F. Mainz, G. Steiner, L. Vazquez, M. T. Pham, R. Salzer, Colloid Surface B: Biointerfaces **42**, 219 (2005).

[4] B. Sivaraman, K. P. Fears, R. A. Latour, Langmuir, **25**, 3050 (2009).

[5] R. A. Latour, Biomaterials: Protein-Surface Interactions, in Encyclopedia of Biomaterials and Biomedical Engineering (eds. Gary L. Bowlin; Gary Wnek), 2005, Informa Healthcare Publ., New York.

[6] S. Lousinian, N. Kalfagiannis, S. Logothetidis, Mat. Sci. Eng. B-Solid **152**, 12 (2008).

[7] G. Clarotti, F. Schue, J. Sledz A.Ait Ben Aoumar, K.E. Geckeler, A. Orsetti,G. Paleirac, Biomaterials, **13**, 832 (1992).

[8] X. Y. Lu, Y. Huang, W. P. Qian, Z. M. Tang, Z. H. Lu, J. Biomed. Mater. Res. **66A**, 722 (2003).

[9] L. Tang, A. H. Lucas, J.W. Eato, J. Lab. Clin. Med. **122**, 292 (1993).

[10] L.F. Steel, M. G. Trotter, P.B. Nakajima, T.S. Mattu, G. Gonye, T. Block, Mol. Cell. Proteomics **2**, 262 (2003).

[11] S. Sugio, A. Kashima, S. Mochizuki, M. Noda, K. Kobayashi, Protein Eng. Des. Sel. **12**, 439 (1999).

[12] J.P. Nicholson, M.R. Wolmarans, G.R. Park, Brit. J. Anaesth. **85**, 599 (2000).

[13] L. Tang L, J. W. Eaton, Am. J. Clin. Pathol. **103**, 466 (1995).

[14] Z. Bai, M.J. Filiaggi, J.R. Dahn, Surf. Sci. **603**, 839-(2009).

[15] V. Balasubramanian, N.K. Grusin, R.W. Bucher, V.T. Turitto, S.M. Slack, J. Biomed. Mater. Res. **44**, 253-60 (1999).

[16] I.D. Xynos, A.J. Edgar, L.D.K. Buttery, L.L. Hench, J.M. Polak, J. Biomed. Mater. Res **55**, 151 (2001).

[17] M. Kawashita, H. Takaoka, T. Kokubo, T. Yao, S. Hamada, T. Shinjo, J. Ceram. Soc. Jpn., **109**, 39 (2001).

[18] V. Simon, S. Cavalu, S. Simon, H. Mocuta, E. Vanea, M. Prinz, M. Neumann, Solid State Ionics, **80**, 764 (2009).

[19] D. Eniu, D. Cacaina, M. Coldea, M. Valeanu, S. Simon, J. Magn. Magn. Mater., **293**, 310-313 (2005).

[20] V. Simon, D. Eniu, A. Gritco, S. Simon, J. Optoelectron. Avd. Mater. **9**, 3368-3371 (2007).

[21] M. Tamasan, T. Radu, S. Simon, I. Barbur, H. Mocuta, V. Simon, J. Optoelectron. Avd. Mater. **10**, 948 (2008).

[22] T. Kokubo, H. Kushitani, S. Sakka, T. Kitsugi, T. Yamamuro, J. Biomed. Mater. Res. **24**, 721 (1990).

[23] M. Advincula, X. Fan, J. Lemons, R. Advincula, Colloid Surface B: Biointerfaces **42**, 29 (2005).

[24] A. P. Serro, M.P. Gispert, M.C.L. Martins, P. Brogueira, R. Colaco, B. Saramago, J. Biomed. Mater. Res. **78A**, 581-589 (2006).

[25] M. M. Browne, G.V. Lubarsky, M.R. Davidson, R. H. Bradley, Surface Science **553**, 155 (2004).

[26] S. Simon, R.V.F. Turcu, T. Radu, M. Moldovan, V. Simon, J. Optoelectron. Avd. Mater. **11**, 1660 (2009).
[27] G. Polzonetti, M.V. Russo, A. Furlani, G. Iucci, Chem. Phys. Lett. **185**, 105 (1991).
[28] G. Reiter, N. Hassler, V. Weber, D. Falkenhagen, U.P. Fringeli, Biochim. Biophys. Acta **1699**, 253 (2004).
[29] G. Falini, E. Foresti, I.G. Lesci, B. Lunelli, P. Sabatino, N. Roveri, Chem. Eur. J. **12**, 1968 (2006).
[30] W. J. Yang, P.R. Griffiths, D.M. Byler, H. Susi, Appl. Spectrosc. **39**, 282 (1985).
[31] D. M. Byler, H. Susi., Biopolymers **25**, 469 (1986).
[32] C. K. Krishnan, Biomaterials **19**, 357 (1998).
[33] J. R. Powell, F.M. Wasacz, R.J. Jakobsen, Appl. Spectrosc. **40**, 339 (1986).
[34] S. Cavalu, V. Simon, J. Optoelectr. Avd. Mater. **9**, 3297 (2007).
[35] S. Cavalu, V. Simon, F. Banica, C. Deleanu, Rom. J. Biophys. **17**, 237 (2007).
[36] W.K. Surewicz, H.H. Mantsch, Biochim. Biophys. Acta, **952**, 115 (1988).
[37] K. K. Chittur, Biomaterials **19**, 357 (1998).
[38] J. Serra, P. Gonzalez, S. Liste, C. Serra, S. Chiussi, B. Leon, M. Perez-Amour, H. Ylanen, M.Hupa, J. Non-Cryst. Solids **332**, 20 (2003).

*Corresponding author: viorica.simon@phys.ubbcluj.ro